DESIGN OF AN ACTIVE SUSPENSION SYSTEM FOR AN AUTOMOBILE

by

GENE M. FIELDS

S.B. Massachusetts Institute of Technology

1972

SUBMITTED IN PARTIAL FULFILLMENT OF THE
REQUIREMENTS FOR THE DEGREE OF
MASTER OF SCIENCE
at the
MASSACHUSETTS INSTITUTE OF TECHNOLOGY

February 1973

Signature of Author Signature redacted
Department of Aeronautics and Astronautics, January 31, 1973

Certified by Signature redacted
Thesis Supervisor

Accepted by Signature redacted
Chairman, Departmental Committee on Graduate Students

DESIGN OF AN ACTIVE SUSPENSION SYSTEM

FOR AN AUTOMOBILE

by

GENE M. FIELDS

Submitted to the Department of Aeronautics and Astronautics on January 31, 1973 in partial fulfillment of the requirements for the degree of Master of Science.

ABSTRACT

In this study an active suspension system is designed employing an electrohydraulic actuator to help isolate the automobile from road vibrations. After an actuator model is derived, its application as a linear active element is investigated. Feedback signals are then optimized to give a desired frequency response. It was found that the transmission of vibrations from the road to the passenger could be substantially reduced by introducing the active element.

For large, discrete disturbances, even at moderate speeds, the tire loses contact with the road. Thus, forces on the body are unsymmetrical with respect to positive and negative steps. In an attempt to maintain zero induced body acceleration due to these disturbances, various nonlinearities are introduced into the actuator, and the system is modeled on the analog computer. By proper adjustment, the nonlinear actuator did, in fact, improve the system response.

Thesis Supervisor: Renwick E. Curry
Title: Assistant Professor of
Aeronautics and Astronautics

ACKNOWLEDGMENTS

The author wishes to thank his thesis supervisor, Professor Renwick E. Curry, for his guidance, encouragement, and patience during the author's studies. Professor H. Philip Whitaker was most helpful and encouraging throughout the course of this study, and the author wishes to recognize his rare quality for encouraging his students.

The author also wishes to thank Yi Cheng, fellow student and friend, for his help throughout the author's graduate work. Finally, thanks are due to my wife, Jemmy, who contributed patience and understanding, and who typed this thesis.

TABLE OF CONTENTS

LIST OF ILLUSTRATIONS

LIST OF SYMBOLS

A	Effective area of actuator ram (in^2)
A	An orifice area (in^2)
B	Shock absorber damping constant (lb-sec/ft)
C, D,	Constant state matrices
J, K	" " "
C_1	Effective damping constant of actuator (lb-sec/ft)
C_2, C_3, C_4,	Feedback gains
C_5, C_6	" "
C_d	Orifice discharge coefficient
C_p, C_x	Valve coefficients (in^5/lb) (in^2/sec)
d	Solenoid damping constant
F	Actuator force (lb)
f_1, f_2, f_b	Tire, suspension, and body force increments (lb)
G	Total gain of linear actuator (lb/ma)
H_1, H_2	Feedback functions
i	Input current to solenoid (ma)
K_1	Tire radial spring constant (lb/ft)
K_2	Spring constant (lb/ft)
k_0	Solenoid gain
k_1	Amplifier gain
L	Leakage coefficient for valve and piston (in^5/lb)
L	Solenoid inductance (henries)
M_1	Mass of wheel and supporting axle (slugs)
M_2	Body mass of single support system (slugs)

m	Mass of solenoid core (slugs)
P_e	Valve exit pressure (lb/in^2)
P_l	Load pressure (lb/in^2)
P_s	Constant supply pressure to actuator (lb/in^2)
ΔP	Pressure drop across an orifice (lb/in^2)
q	Volumetric flow rate (in^3/sec)
q_l	Load flow rate (in^3/sec)
R	Solenoid and amplifier output resistance (ohms)
s	Laplace operator
T_e	Eddy current time constant (sec)
U	Valve spool underlap (in)
u	State vector input
V	Actuator fluid volume (in^3)
x	Valve spool displacement (in)
x_0	Deviation of the road surface (in)
x_1	Axle displacement (in)
x_2	Body displacement (in)
Y	Actuator ram displacement (in)
y	State vector output
Z	State vector
$\dot{Z}$	dz/dt
β	Bulk modulus of fluid (lb/in^2)
Δ	A small increment
ρ	Density of fluid ($lb\ sec^2/in^4$)

LIST OF SYMBOLS (continued)

τ	Time constant of actuator (sec)
ξ	Damping ratio
ω_1	Body natural frequency (rad/sec)
ω_2	Wheel-bounce natural frequency (rad/sec)

CHAPTER I

INTRODUCTION

An automobile suspension system is designed to reduce the transmission of random vibrations of road disturbances to the body frame and passengers, without excessive loss of control of the vehicle during manuvering. By keeping the vehicle-to-road contact as high as possible, one insures good control, both in stopping and turning. This, however, presents a greater requirement of the suspension system in isolating road disturbances from the passenger. Existing systems employ only passive elements; that is, no external energy sources. The essential features of this type of suspension are a load supporting member in the form of a spring, and some form of damper to dissipate energy. The principal limitation in passive suspension systems is that the bandwidth cannot be decreased without reducing the stiffness of the supporting member. Since the static deflection varies as the inverse square of the natural frequency in a passive system(1), a severe constraint is formed due to the maximum body deflection which can be tolerated. One may therefore conclude that the suspension system may be improved by introducing an active vibration isolator or nonlinearities. This is essentially a servomechanism, operated by command signals from continuous feedback information. Sensing elements provide signals proportional to quantities such as the acceleration, rate, or position of some point in the system. These signals are modified and combined to form a command signal which drives some type of force actuator. When, for example, the wheel experi-

ences a sudden dip or bump, an acceleration is generated through the system. If this condition can be sensed, then signals can be sent to the actuator to extend or contract the position of the wheel relative to the position of the body. Therefore, the tire can maintain contact with the road at all times and the body will experience a minimum of transmitted jerk and acceleration. Of course, at high frequencies this condition will break down due to obvious physical constraints.

In considering a one-dimensional model, the existing suspension system can be modeled as a three-stage mechanical filter. This consists of a spring for the forst stage in the form of a tire, a spring and damper for the second stage which is employed between the axle and automobile body, and effectively a spring and damper in the form of the cusioned seat. The first and second stages, of course, absorb the greatest vibration. It is desired then, to optimize the suspension system in the first two stages and the dynamics of the seat will therefore not be included. For this study, it is sufficient to consider a simplified model consisting of a single tire, a spring and damper, and the portion of the body associated with each tire. (Fig. 1)

Previous work on the problem of active suspension has included various types of control. The air bag suspension of commercial buses and other types of height correction methods have been investigated. These basically involved inputs of relative axle-to-body displacements to the control element. Panzer(2) develops the theory and design of active suspensions, but does not complete the synthesis of the actual hardware. Bender(3) has presented an analysis employing random process theory in the design of an optimum suspension system.

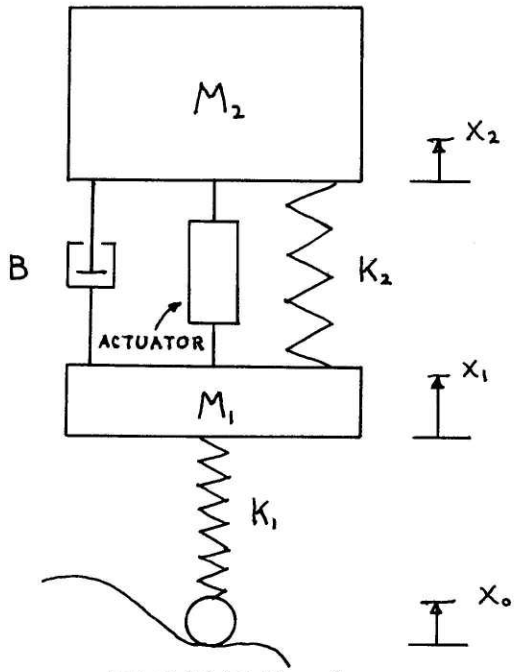

FIGURE 1

Thompson (4)(5) has studied the theory of active, passive, and optimal nonlinear suspensions. In (4), he has effectively employed a dynamic vibration absorber to isolate the road disturbances at the undamped wheel-bounce natural frequency. This device consisted of a small mass, spring, and damper tuned to the wheel-bounce frequency to absorb maximum energy at that value. Although this method adequately isolates road disturbances, this study will investigate the feasibility of handling this high frequency vibration through the actuator. By employing feedbacks, which are functions of the axle motion as well as the body motion, one can provide phase lead information to the actuator concerning the high frequency wheel-bounce forces being generated. The objective then, is to design an actuator with a time response short enough to accurately carry out the commands provided

by the sensing elements. The design problems will be kept within the constraints of being physically realizable, and employing existing components.

The dynamics of the automobile are, of course, the initial constraint. The excitations experienced by an automobile arise from road irregularities and external forces acting on the vehicle. The road disturbances are essentially random in nature (1). External forces are due to such conditions as body aerodynamics, excess weight in the vehicle, changes in the grade, or turning manuevers. Although these excitations are both translational and rotational in all axes of the vehicle, only vertical components will be considered for the purposes of vibration isolation.

From Fig. 1, the following differential equations of motion may be derived in terms of the Laplace operator S.

$$F_2 - F_b = M_2 S^2 X_2 \tag{1.1}$$

$$F_1 - F_2 = M_1 S^2 X_1 \tag{1.2}$$

$$F_1 = K_1(X_0 - X_1) \tag{1.3}$$

$$F_2 = (K_2 + BS)(X_1 - X_2) \tag{1.4}$$

where

F_1 = Tire force

F_2 = Spring and damper force

F_b = Body force

K_1, K_2 = Spring constants

M_1, M_2 = Wheel and body masses

B = Damping constant

X_0, X_1, X_2 = Road, axle and body displacements measured at static equilibrium

Solving for the accelerations of the axle and body, one obtains

$$S^2 X_2 = (X_1 - X_2) K_2/M_2 + (X_1 - X_2) BS/M_2 \tag{1.5}$$

$$S^2 X_1 = -(X_1 - X_2) K_2/M_1 - (X_1 - X_2) BS/M_1 + (X_0 - X_1) K_1/M_1 \tag{1.6}$$

These may be rearranged to give the block diagram of Fig. 2., where the road deflection X_0 is considered the input and the body force F_b, the sum of the external disturbances. Since certain elements of the suspension are error-actuated, it operates similarly to a position-control feedback system. It is evident that the first loop contains an almost undamped natural frequency of $\sqrt{K_1/M_1}$ due to the tire. The design difficulties due to this constraint are further increased due to the fact that any design of active control directly in this loop would involve practical difficulties in realization, since neither X_1 nor X_2 could be accurately measured with respect to X_0.

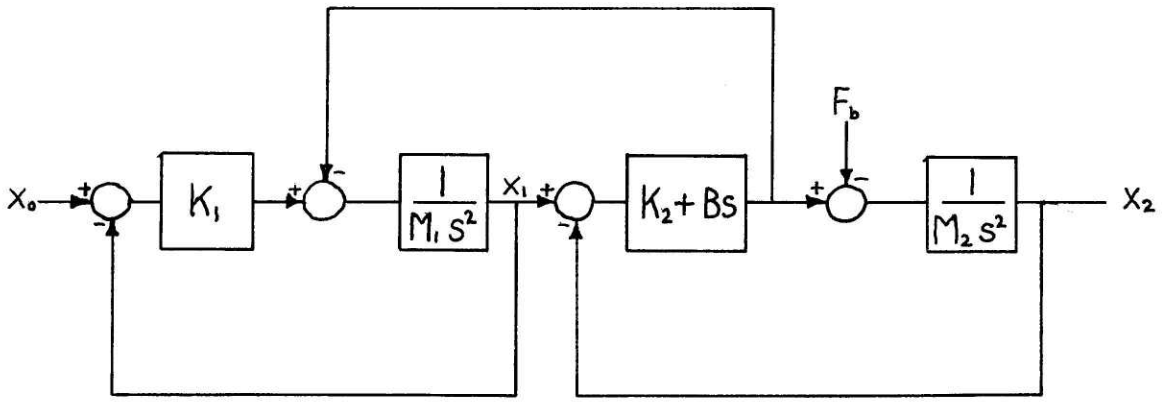

FIGURE 2

One is then forced to choose the location of the active force compensation element in the second loop or effectively between the body and axle, as are the existing spring and damper.

This study will investigate the type of controller which could best meet the design requirements from a practical point of view. The controller must then be designed along with the proper choice of actuating signals. First, a design will be investigated employing a linear model for the actuator, then a nonlinearity will be introduced in order to provide unsymmetrical counter forces for excessively large positive and negative step inputs. Various feedbacks and nonlinear forms are investigated in an attempt to maintain zero body acceleration from reference upon undergoing severe disturbances. The automobile body would then ride at a relatively constant inertial position for an unsloped terrain. For the linear analysis, a system description program to factor high order transfer functions and a parameter optimization program to choose optimum feedback gains and actuator characteristics were employed on the IBM 370 computer. The system was then modeled on the analog computer to carry out the nonlinear study.

CHAPTER II

PROBLEM FORMULATION AND DESIGN CRITERION

The level of desired vibration isolation is subjective in nature, but is dependent on human comfort as well as the prevention of damaging effects to equipment. It is, therefore, very difficult to define the degree of vibration isolation which the passenger accepts as a comfortable ride. Investigations have been made in this area, and the S.A.E. (6) has published a set of transmission limits of vertical vibration for human comfort which the author will use as a basis for design. These limits for a sinusoidal road of one inch amplitude, are given in Fig. 3. For comparison, the frequency response of the automobile must be plotted.

From the differential equations of Chapter I, the following transfer functions between axle deflection and road; and body deflection and road may be obtained:

$$\frac{X_1}{X_0} = \frac{M_2K_1s^2 + BK_1s + K_1K_2}{M_1M_2s^4 + (M_1+M_2)Bs^3 + (M_1K_1 + M_2K_2 + M_2K_1)s^2 + BK_1s + K_1K_2} \tag{2.1}$$

$$\frac{X_2}{X_0} = \frac{K_1Bs + K_1K_2}{M_1M_2s^4 + (M_1+M_2)Bs^3 + (M_1K_1 + M_2K_2 + M_2K_1)s^2 + BK_1s + K_1K_2} \tag{2.2}$$

Actual values for the masses, spring constants, and damping constant vary greatly of course, but the following fixed parameter values are typical of an automobile (4) and are hereby assumed.

Body mass M_2	20 slugs
Wheel mass M_1	2 slugs
Spring constant K_2	1370 lb/ft
Tire radial spring constant K_1	10680 lb/ft
Shock absorber damping rate B	136 lb-sec/ft

With these values, equations 2.1 and 2.2 become:

$$\frac{X_1}{X_0} = \frac{10{,}680(20S^2 + 136S + 1370)}{40S^4 + 2{,}992\,S^3 + 262{,}360\,S^2 + 1{,}451{,}480S + 14{,}631{,}480} \tag{2.3}$$

and

$$\frac{X_2}{X_0} = \frac{10680(136S + 1370)}{40S^4 + 2{,}992\,S^3 + 262{,}360\,S^2 + 1{,}451{,}480S + 14{,}631{,}480} \tag{2.4}$$

By factoring into the characteristic roots, the frequency response of Fig. 3. may be obtained.

It is evident, that there are two natural frequencies in this system associated with each of the two feedback loops in Fig. 2. From the plot of Fig. 3. a great reduction in the amplitude ratio at the natural wheel-bounce frequency, along with added damping in both loops, is desired. This design criterion will be applied to the linear study with random road disturbances over a frequency range to 10^3 rad/sec. However, for discrete disturbances such as step inputs, the integral-square body acceleration will be minimized.

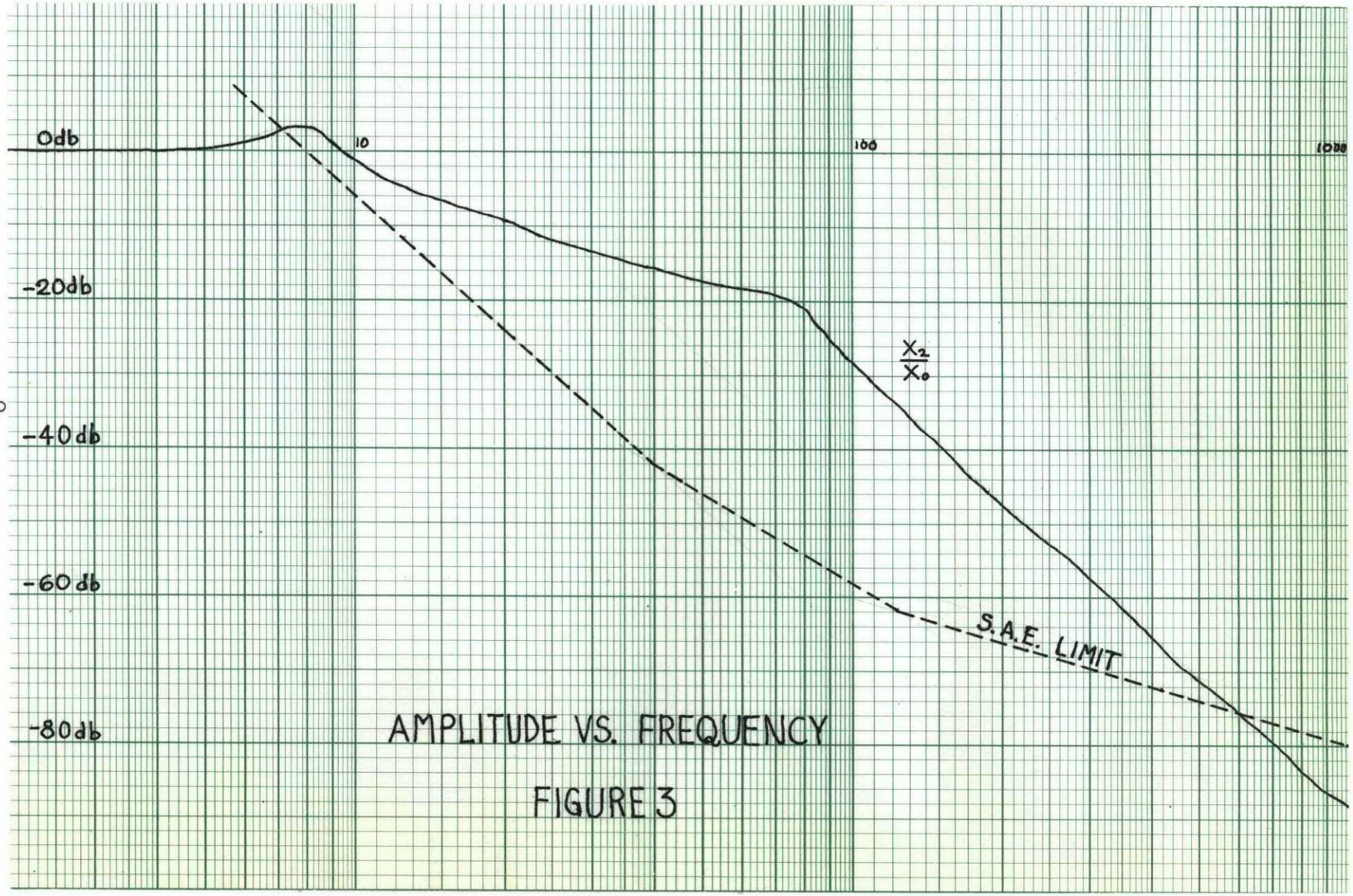

AMPLITUDE VS. FREQUENCY

FIGURE 3

CHAPTER III

ACTUATOR MODEL

The various types of actuators that may be used for vibration isolation include mechanical (rack and pinion mechanisms), and fluidic (pneumatic or hydraulic) elements. Mechanofluidic systems are relatively uncomplicated, but the types of pure mechanical sensors which would be practical for this application limit them somewhat. Electrofluidic mechanisms, though more complex, have the ability to meet more demanding constraints. Therefore, a fluidic actuator with electronic feedback was chosen for this design. The choice of a pnuematic or a hydraulic actuator to best meet the design criterion must also be made. Even before further investigation of the specific requirements of the actuator, one may list several disadvantages of using a pnuematic medium. Nonlinear flow characteristics, temperature sensitivity, and high compressibility may change the effective forces generated by the actuator and influence stability. (8) On the other hand, possibly more energy could be absorbed in the actuator than transmitted through to the body with a more compressible medium. Thus, in the case of air cushioned springs, pnuematic power is well suited. However, the hydraulic system is chosen for this design on the basis of the disadvantages associated with a pnuematic medium.

There are, of course, many different designs in electrohydraulic actuators. A linear actuator used for the initial design in this study

consists of flow control against a piston surface, through variable orifices in order to provide the necessary forces. By varying the orifice sizes, the desired relationship between pressure drop and flow may be obtained (7) from

$$q = C_d A' \sqrt{\frac{2\Delta P}{\rho}} \tag{3.1}$$

where q = orifice volumetric flow rate
C_d = coefficient of discharge
A' = orifice area
ΔP = pressure drop
ρ = density of the fluid.

Valve characteristics are therefore nonlinear; however, they are commonly linearized around an operating point providing the displacements are small.

In considering the choice of control valve configuration for this application, both the spool-type and the flapper-nozzle valve have appeal. The flapper-nozzle valve has certain mechanical design advantages. Construction is simpler and the lack of close-clearance sliding parts eliminates friction forces in the valve. However, the fact that they are generally limited to lower pressure applications due to their continuous flow principle could introduce difficulties. Three-way valves are simpler in construction, but exhibit less symmetry in operation. Generally, they have lower flow gains, and are much less linear over a specified range than a four-way design. (8) Since, as a further investigation of isolating excessively large bumps or dips, the use of unsymmetrical force characteristics will be studied, it was decided to employ a spool-type, four-way constant-pressure control valve. Its symmetry offers the

designer a more predictable model with which to control and observe the nonlinearity. With these choices, a model must now be chosen.

An actuator model similar to the one used in this study has been developed in several texts (8) and publications (9). A diagram of the actuator is shown in Fig. 4. Since the actuator will be placed in a paralell arrangement with the spring and damper, it must be an open center spool valve. This provides for a continuous flow through the spool. The compressibility of the fluid contributes a slight damping effect, but is negligible compared to the shock absorber for the small volumes associated with the actuator. A closed center design would therefore act as a near rigid strut between the body and axle. The

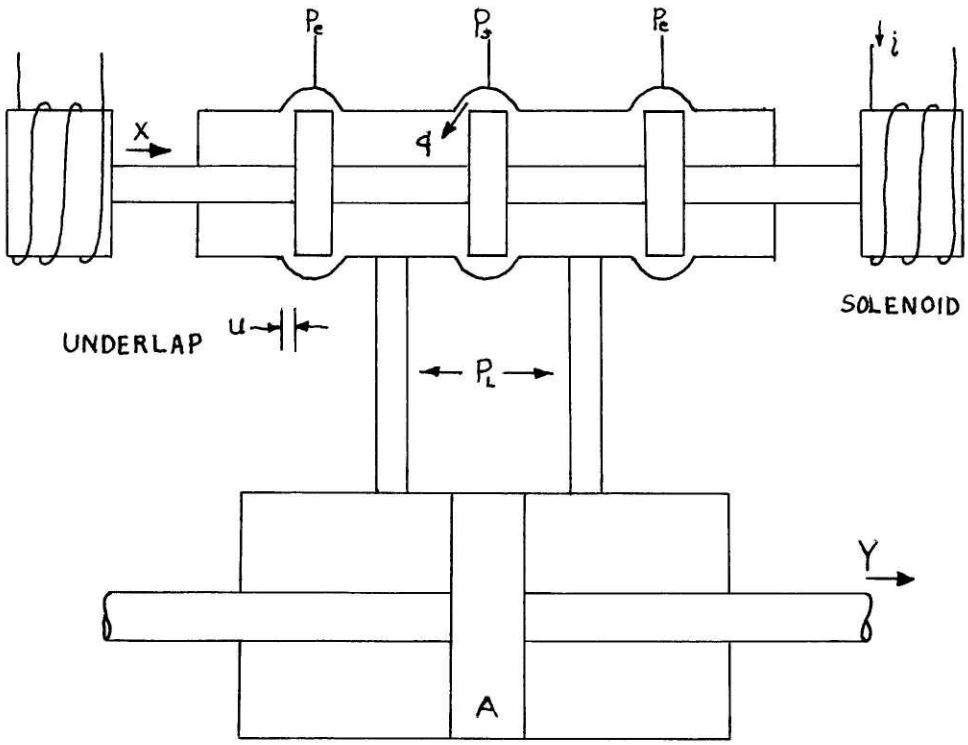

FIGURE 4

characteristics of the actuator are of course very sensitive to this underlap. For example, the effective damping constant may be decreased to a physically meaningful value with a proper choice of underlap; however, changes in flow become more sensitive to load pressure variations. Obviously an optimum value exists, once constraints and desired performance characteristics are determined.

To proceed further, a mathematical model of the actuator dynamics must be obtained. The following assumptions are made in modeling the dynamics of the actuator: (8)

1. All damping forces are viscous in nature; and coulomb friction has been neglected.
2. Viscous leakage flows are neglected.
3. Head losses in the fluid passages are negligible.
4. Both steady and unsteady flow forces are included in the effective spring and damping constants.
5. Load forces are small compared to the actuator force.

Linearized equations may now be written governing the flows and forces in the valve and ram.

Proportional control valves require a complete family of curves to describe their operation. Because the flow through the valve is both a function of the valve opening and the load pressure, relationships for the gradients of the characteristic curves must be obtained. For constant load pressure, a small change in the flow ΔQ corresponds to a small change in the valve opening ΔX. This gives rise, in the limit, to the flow gradient $(\partial Q/\partial X)_o$. Similarly with constant X, the leakage gradient which is a function of the valve spool underlap parameter becomes $(\partial Q/\partial P_L)_o$.

Therefore, the flow through the valve q, the displacement of the valve spool x, and the load pressure P_L, measured from reference points of zero, are related by the following: (8)

$$q = \left(\frac{\partial q}{\partial x}\right)_{P_L} x + \left(\frac{\partial q}{\partial P_L}\right)_x P_L \tag{3.2}$$

Defining

$$C_x = \left(\frac{\partial q}{\partial x}\right)_0 \tag{3.3}$$

and

$$C_p = -\left(\frac{\partial q}{\partial P_L}\right)_0 \tag{3.4}$$

the valve spool flow equation becomes

$$q = C_x x - C_p P_L \tag{3.5}$$

where the partial derivatives C_x and C_p are obtained from the valve pressure-flow characteristic curves at the operating point. A typical set of curves for an open center spool valve (8) is shown in Fig. 5.

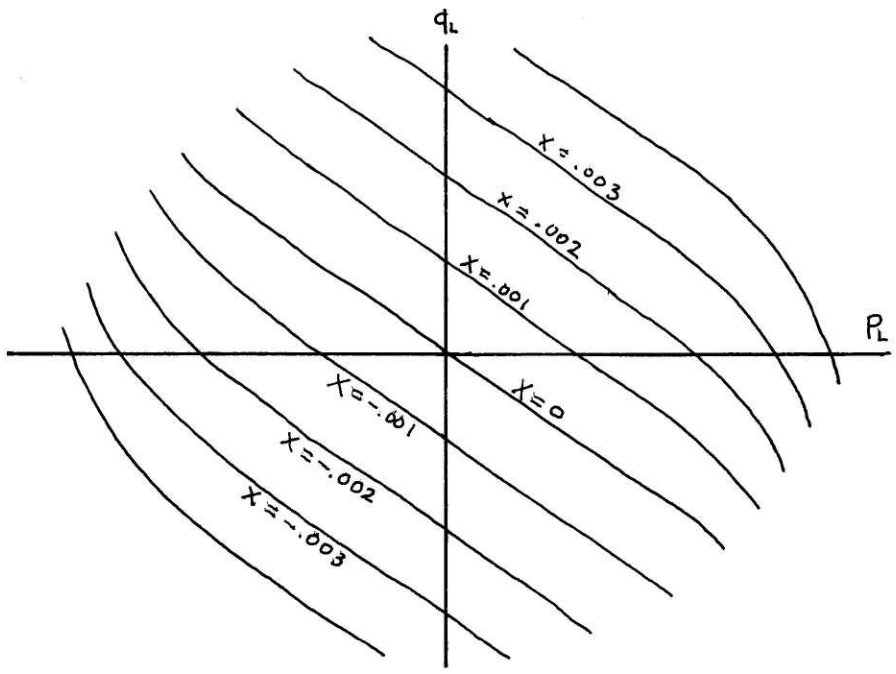

FIGURE 5

The ram flow equation may now be derived by considering the total flow as a sum of compressible, incompressible, and leakage components. Since the actuator will operate under relatively large forces, and valve response time is very important; the compressibility of the fluid must be considered. For a volume V of fluid in a cylinder, the phenomenon of compressibility can be expressed by the bulk modulus

$$\beta = \rho \frac{dP}{d\rho} \tag{3.6}$$

where P is the pressure on the fluid with density ρ. The variation in density of a typical hydraulic fluid for the commonly encountered pressure changes is small and will be neglected, but the rate of change of density may be quite large compared to the other quantities, and therefore must be considered.(8) Thus, equation 3.6 may be written as

$$\frac{dP_L}{dt} = \frac{\beta dV}{V dt} \tag{3.7}$$

or equivalently

$$q_c = sP_L \frac{V}{\beta} \tag{3.8}$$

where s is the Laplace operator $\frac{d}{dt}$. The leakage flow past the ram may be expressed as

$$q_\ell = LP_L \tag{3.9}$$

where L, the leakage flow coefficient in $in^5/lb\text{-}sec$, is a function of the geometry of the actuator. The load velocity flow or incompressible component is given by

$$q_o = AsY \tag{3.10}$$

where Y is a small change in the ram displacement, and A is the effective area. This results in a total ram flow of

$$q = sP_L\frac{V}{\beta} + LP_L + sYA \tag{3.11}$$

Since the valve flow and ram flow must be equal,

$$C_x X - C_p P_L = sP_L\frac{V}{\beta} + LP_L + sYA \tag{3.12}$$

Neglecting the external forces on the ram gives a force developed by the actuator of

$$F = AP_L \tag{3.13}$$

Combining equation 3.12 and equation 3.13 gives

$$sF = -\frac{sA^2Y\beta}{V} - (L+C_p)\frac{\beta}{V}F + \frac{C_xA\beta}{V}X \tag{3.14}$$

If an arrangement of solenoids is used to drive the spool valve, as shown in Fig. 4, the input must be in the form of a current. However, the valve input is a displacement. In relating these two, the following transfer function is written as (7)

$$\frac{X}{I} = \frac{k_o}{(T_e s+1)(L'/R\,s+1)(m/k_1 s^2 + d/k_1 s + 1)} \tag{3.15}$$

where

T_e = Eddy current time constant
L' = Inductance
m = Mass of solenoid core
k_1 = Amplifier gain
d = Effective damping constant
k_o = Solenoid gain
R = Solenoid and amplifier output resistance

For small control valves, the solenoid gain typically varies between 0.0002 and 0.0008 in/ma; and the maximum displacement is approximately

$\pm$ 0.015 in. The L'/R time constant may be neglected for high - impedance systems employing an electronic amplifier in the drive circuit. (7) This subsequently proves applicable, due to the relatively high feedback gains required.

Since the natural frequency of typical small solenoids for such an application are above 100 Hz, and experimental results (7) have shown in d.c. applications that T_e is usually below 10^{-3}, the dynamics at these frequencies may be neglected. The solenoid often contains a dead band and other nonlinearities, but operation in a push-pull manner generally helps maintain more linear and symmetric characteristics. Dead band nonlinearities lead to possible steady state errors, but such effects are assumed to be small here. Therefore, the relation of the input current to the valve spool deflection will be modeled as a constant k_o, provided frequencies of concern are below 10^3 rad/sec.

CHAPTER IV

LINEAR ACTIVE SUSPENSION

Having formulated a dynamic model of the actuator, one may now proceed to the problems of integrating it with the suspension system. Both actuator parameters and driving signals from the sensors are dependent upon the characteristics of the system to be controlled. The use of functional block diagrams clearly show the transmission of signals, displacements, and forces; and offer a good place to begin.

As planned, the ram drive is connected to the axle and the actuator housing to the body frame. Since the ram deflection Y is measured relative to the actuator housing, it is equivalent to the difference between the body and axle deflections $X_2 - X_1$. Thus, equation 1.4 is rewritten to include the contribution due to the actuator force.

$$F_2 = (K_2 + BS)(X_1 - X_2) + F \tag{4.1}$$

Combining equations 1.5, 1.6, 3.14, and 4.1, the system may now be described by

$$S^2 X_2 = (X_1 - X_2)(K_2/M_2 + B/M_2 S) + F/M_2 \tag{4.2}$$

$$S^2 X_1 = -(X_1 - X_2)(K_2/M_2 + B/M_2 S) + (X_0 - X_1)K_1/M_1 - F/M_1 \tag{4.3}$$

$$F(\tau S + 1) = -SYC_1 + iG \tag{4.4}$$

where

$$\tau = V/(L + C_p)\beta \tag{4.5}$$

$$G = C_x A k_o \tau \beta / V \tag{4.6}$$

$$C_1 = A^2 \tau \beta / V \tag{4.7}$$

This gives rise to a new block diagram containing the external force generation from the actuator. (Fig. 7.) One of the major problems in this study then, results in the choice of signals to actuate the controlling element. Since the only practical measurements for feedback would involve either functions of X_1, or X_2, or possibly functions of their difference, a very general feedback scheme may be adopted in the following form. (Fig. 8.) Clearly, from equation 4.2, the road induced accelerations in the body can be substantially decreased by applying negative displacement feedback. Its contribution then opposes the spring force $K_2/M_2(X_2 - X_1)$.

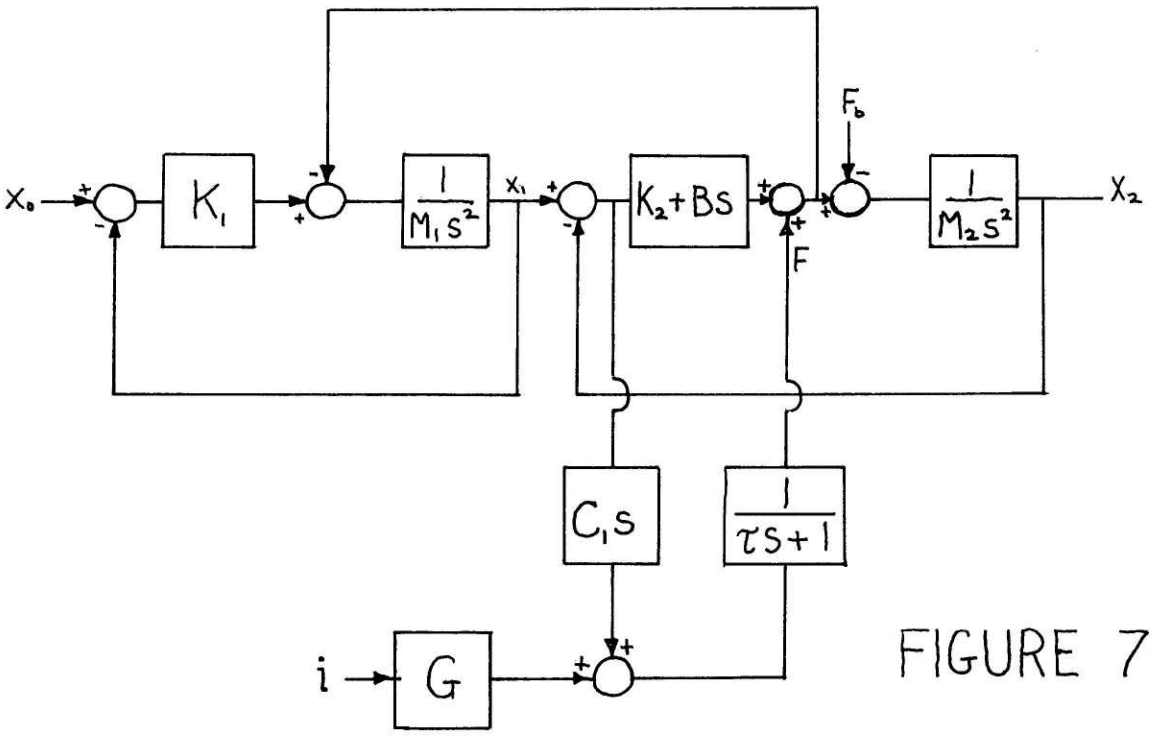

FIGURE 7

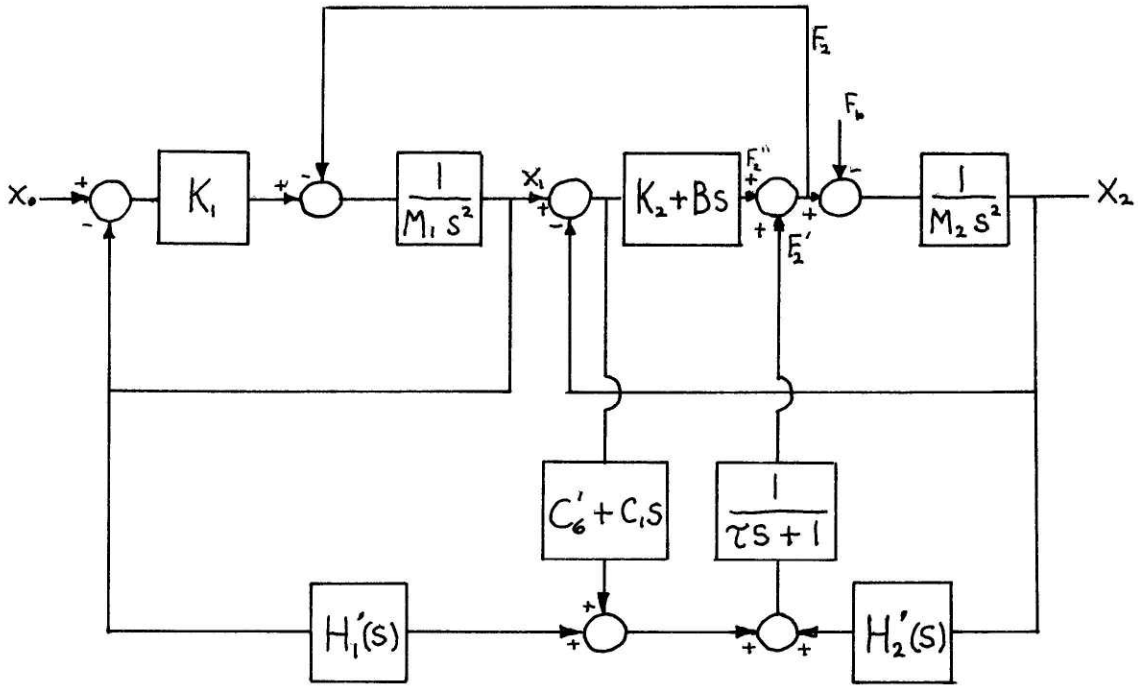

FIGURE 8

Therefore by defining

$$H_1(s) = H_1'(s)/(\tau s+1) \tag{4.8}$$

$$H_2(s) = H_2'(s)/(\tau s+1) \tag{4.9}$$

$$C_6 = C_6'/(\tau s+1) \tag{4.10}$$

the following equations may be obtained:

$$F_1 - F_2 = M_1 s^2 X_1 \tag{4.11}$$

$$F_2 = F_2' + F_2'' \tag{4.12}$$

$$F_2'' = \left(K_2 + Bs + C_1 s/(\tau s+1)\right)(X_1 - X_2) \tag{4.13}$$

$$F_2' = H_1(s)\,X_1 + H_2(s)\,X_2 - C_6(X_1 - X_2) \tag{4.14}$$

$$F_1 = K_1(X_0 - X_1) \tag{4.15}$$

$$F_2 - F_b \simeq M_2 s^2 X_2 \tag{4.16}$$

From these, the following transfer functions between axle and road, and body and road may be obtained:

$$\frac{X_1}{X_0} = \frac{b_2 s^2 + b_1 s + b_0}{a_4 s^4 + a_3 s^3 + a_2 s^2 + a_1 s + a_0 + h} \tag{4.17}$$

$$\frac{X_2}{X_0} \simeq \frac{c_2 s^2 + c_1 s + c_0}{a_4 s^4 + a_3 s^3 + a_2 s^2 + a_1 s + a_0 + h} \tag{4.18}$$

where

$$\begin{aligned}
b_2 &= M_2 K_1 \\
b_1 &= K_1(B + C_1/\tau s + 1) \\
b_0 &= K_1(K_2 - H_2(s) - C_6/\tau s + 1) \\
c_2 &= b_1/s \\
c_1 &= K_1/s\,(K_2 - C_6/\tau s + 1) \\
c_0 &= K_1\,H_1(s) \\
a_4 &= M_1 M_2 \\
a_3 &= (M_1 + M_2)(B + C_1/\tau s + 1) \\
a_2 &= ([M_1 + M_2][K_2 - C_6/\tau s + 1] + M_2 K_1) \\
a_1 &= b_1 \\
a_0 &= K_1(K_2 + C_6/\tau s + 1) \\
h &= (M_2 H_1(s) - M_1 H_2(s))s^2 - K_1 H_2(s)
\end{aligned}$$

The feedback functions H_1 and H_2 must now be chosen with respect to the frequency and damping in the two loops in an attempt to attain the desired system response.

To establish the provision for observing the response with acceleration and rate information, the feedback functions are initially chosen as

$$H_1(X_1) = C_2 S^2 + C_3 S \tag{4.19}$$

$$H_2(X_2) = C_4 S^2 + C_5 S \tag{4.20}$$

with the parameter values to be determined to give optimum system response. Substitution into equation yields a road to body transmission of

$$\frac{X_2}{X_0} = \frac{K_1 \quad b_2 S^2 + b_1 S + b_0}{a_5 S^5 + a_4 S^4 + a_3 S^3 + a_2 S^2 + a_1 S + a_0} \tag{4.21}$$

where

$$\begin{aligned}
b_2 &= 136\tau + C_2 \\
b_1 &= 136 + 1370\tau + C_1 + C_3 \\
b_0 &= 1370 - C_6 \\
a_5 &= 40\tau \\
a_4 &= 40 + 2992\tau + 20C_2 - 2C_4 \\
a_3 &= 2992 + 22C_1 + 243,740\tau + 20C_3 - 2C_5 \\
a_2 &= 243,740 + 1,452,480\tau - 22C_6 - 10,680C_4 \\
a_1 &= 1,451,480 + 10,680C_1 + 14,631,600\tau - 10,680C_5 \\
a_0 &= 14,631,600 - 10,680C_6
\end{aligned}$$

Obviously, the transfer function must be refactored for each successive trial of parameter values. Therefore a system description program, developed at the M.I.T. Measurement Systems Laboratory (10) by Prof. H. Philip Whitaker was employed. The program, written in FORTRAN IV, permits description of a linear control system, by data input, in the form of elementary transfer functions. One element being multi-input and designated as the controlled member (CONMEM), is described by its

state equations. The program prints transfer functions for designated outputs, the characteristic equation coefficients, state equations, and the factored poles and zeros. Since there is a limit of fifteen individual elements in the description, the CONMEM may be formed to completely describe the plant or existing system before active control is applied. The state equation vectors may be written (11) as

$$\dot{\underline{z}} = J\underline{z} + K\underline{u} \tag{4.22}$$

$$\underline{y} = C\underline{z} + D\underline{u} \tag{4.23}$$

where

$\underline{z}$ = 4 dimensional state vector
$\underline{u}$ = 2 dimensional input vector
$\underline{y}$ = 6 dimensional output vector

and J, K, C, and D are constant matrices. Equations 4.2 and 4.3 may be written in the state vector form by defining

$$z_1 = x_1 \tag{4.24}$$

$$z_2 = \dot{x}_1 \tag{4.25}$$

$$z_3 = x_2 \tag{4.26}$$

$$z_4 = \dot{x}_2 \tag{4.27}$$

$$u_1 = x_0 \tag{4.28}$$

$$u_2 = F \tag{4.29}$$

Taking the first derivative and substituting yields

$$\dot{z}_1 = z_2 \tag{4.30}$$

$$\dot{z}_2 = \ddot{x}_1 = (x_2 - x_1)K_2/M_1 + (\dot{x}_2 - \dot{x}_1)B/M_1 + (x_0 - x_1)K_1/M_1 - F/M_1 \tag{4.31}$$

$$\dot{Z}_3 = Z_4 \tag{4.32}$$

$$\dot{Z}_4 = \ddot{X}_2 = -(X_2 - X_1)K_2/M_2 - (\dot{X}_2 - \dot{X}_1)B/M_2 + F/M_2 \tag{4.33}$$

Since X_1, X_2, and their first and second derivatives are all quantities of interest, the output vector is defined

$$y_1 = X_1 \tag{4.34}$$
$$y_2 = \dot{X}_1 \tag{4.35}$$
$$y_3 = \ddot{X}_1 \tag{4.36}$$
$$y_4 = X_2 \tag{4.37}$$
$$y_5 = \dot{X}_2 \tag{4.38}$$
$$y_6 = \ddot{X}_2 \tag{4.39}$$

The CONMEM may now be expressed in matrix form as

$$\begin{bmatrix} \dot{Z}_1 \\ \dot{Z}_2 \\ \dot{Z}_3 \\ \dot{Z}_4 \end{bmatrix} = \begin{bmatrix} 0 & 1 & 0 & 0 \\ -\frac{K_2+K_1}{M_1} & -\frac{B}{M_1} & \frac{K_2}{M_1} & \frac{B}{M_1} \\ 0 & 0 & 0 & 1 \\ \frac{K_2}{M_2} & \frac{B}{M_2} & -\frac{K_2}{M_2} & -\frac{B}{M_2} \end{bmatrix} \begin{bmatrix} Z_1 \\ Z_2 \\ Z_3 \\ Z_4 \end{bmatrix} + \begin{bmatrix} 0 & 0 \\ \frac{K_1}{M_1} & -\frac{1}{M_1} \\ 0 & 0 \\ 0 & \frac{1}{M_2} \end{bmatrix} \begin{bmatrix} X_0 \\ F \end{bmatrix} \tag{4.40}$$

$$\begin{bmatrix} y_1 \\ y_2 \\ y_3 \\ y_4 \\ y_5 \\ y_6 \end{bmatrix} = \begin{bmatrix} 1 & 0 & 0 & 0 \\ 0 & 1 & 0 & 0 \\ -\frac{K_1+K_2}{M_1} & \frac{-B}{M_1} & \frac{K_2}{M_1} & \frac{B}{M_1} \\ 0 & 0 & 1 & 0 \\ 0 & 0 & 0 & 1 \\ \frac{K_2}{M_2} & \frac{B}{M_2} & -\frac{K_2}{M_2} & -\frac{B}{M_2} \end{bmatrix} \begin{bmatrix} Z_1 \\ Z_2 \\ Z_3 \\ Z_4 \end{bmatrix} + \begin{bmatrix} 0 & 0 \\ 0 & 0 \\ \frac{K_1}{M_1} & -\frac{1}{M_1} \\ 0 & 0 \\ 0 & 0 \\ 0 & \frac{1}{M_2} \end{bmatrix} \begin{bmatrix} X_0 \\ F \end{bmatrix} \tag{4.41}$$

A functional block diagram for use with the system description program may now be drawn. (Fig. 9.)

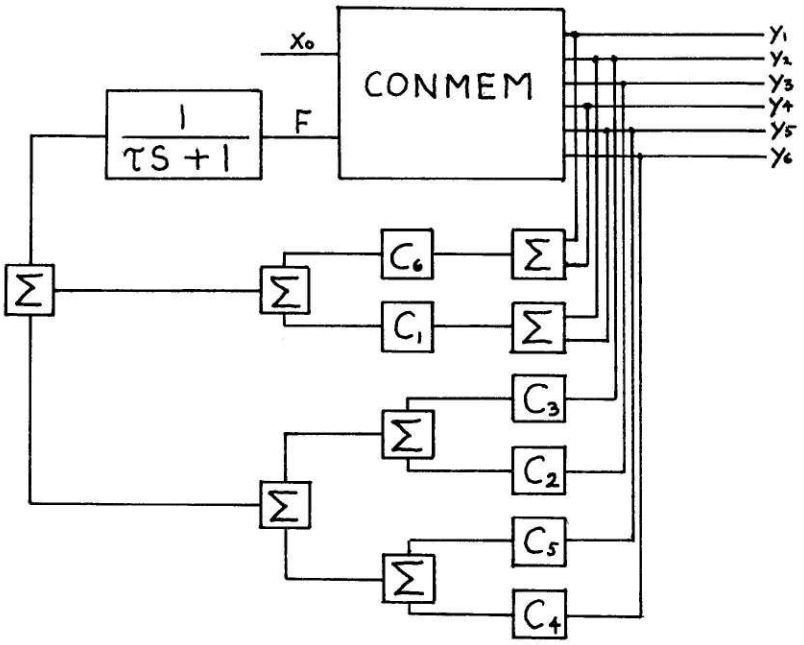

FIGURE 9

For initial choice of parameter values, some advantage can be made of the fact that the natural frequencies are relatively far apart. The low frequency component, at $\omega_1 = 8.3$ rad/sec, is the predominant contribution to equation 4.21 for $\omega \ll \omega_2$. Although an existing root of the numerator has a low break frequency; for low frequencies, the denominator of equation 4.21 becomes approximately

$$\frac{243,740 + 1452,480\,\tau - 22\,C_6 - 10,680\,C_4}{14,631,600 - 10680\,C_6} S^2 + \frac{1.451,480 + 10,680\,(C_1 - C_5) + 14,631,600}{14,631,600 - 10680\,C_6} S + 1 \qquad (4.42)$$

A typical valve for the actuator time constant is .005, and to avoid excessive steady state damping, C_1 is chosen at 50 to be well below the

shock absorber damping rate B. First considering C_4 and C_6 to be zero, a resulting frequency of approximately 7.6 rad/sec, and an adequate damping ratio near .8, may be obtained by choosing $C_5 = -80$. Since the high frequency component is expected to present the greatest difficulty, the remaining parameters will be chosen in an attempt to achieve its desired characteristics.

Although one might simply choose parameter values to reduce the natural frequency and increase the damping of the high frequency component, the second order numerator must first be considered. Increasing the low frequency root, decreases the high frequency root, therefore, it was decided to take advantage of the fact that the second order numerator may be altered by proper feedback parameters to partially cancel the effect of the wheel-bounce component. That is, the numerator frequency is forced to equal ω_2, and the other parameters optimized to yield the closest possible match in damping. The low damped overshoot in the high frequency component may then be decreased by a corresponding undershoot in the numerator. For a frequency of approximately 73 rad/sec and a damping ratio of .3, the proper numerator coefficients may be obtained with $C_2 = -.5$, $C_3 = -185$, and $C_6 = 970$.

It becomes evident at this point, that although negative values of C_2 and C_3 contribute to the desired numerator characteristics, they substantially decrease the damping in the high frequency system. Moreover, the low frequency system is quite sensitive to certain parameter changes in the high frequency system. The task of obtaining even near optimum valves for the seven parameters is indeed complex. Therefore, the use of a computer program was employed which minimizes the mean squared

error between the performance of a control system and a model through its time response. The program employed was based on a PhD. thesis in the Aeronautics and Astronautics Department of M.I.T. by T. Palsson, with revisions by Prof. H. Philip Whitaker. A quadratic performance index defined in terms of the system state vector is minimized with respect to designated free design parameters in a fixed configuration. The system is described as in the previous program.

From the S.A.E. frequency response limits of Fig. 3., a model possessing the desired characteristics, was chosen to be

$$\frac{X_2}{X_0} = \frac{s^2 + 120s + 3200}{s^5 + 130.5s^4 + 7,784s^3 + 147,000s^2 + 1,051,000s + 2,400,000} \qquad (4.43)$$

Since the possible combinations of parameter values is near infinite, it was decided to begin by first considering all feedback gains to be zero and optimizing the two actuator parameters. The effective damping constant C_1, and the time constant τ, were therefore initially optimized to 84 lb sec/ft and .0012 sec respectively. Then introducing the position difference between the two masses (C_6), and the rate of deflection of the axle (C_3), the system subsequently moved nearer to optimum. The frequency response, with these optimized parameter values, is plotted in Fig. 10., and the time response in Fig. 11. Since the response of the system is predominantly due to the low frequency contribution, there exists a good match with the model in the time domain. However, the high resonant peak overshoot in Fig. 10. does not greatly affect the time response of the system, and the effectiveness of the optimization procedure is much less in attaining proper high frequency characteristics. However,

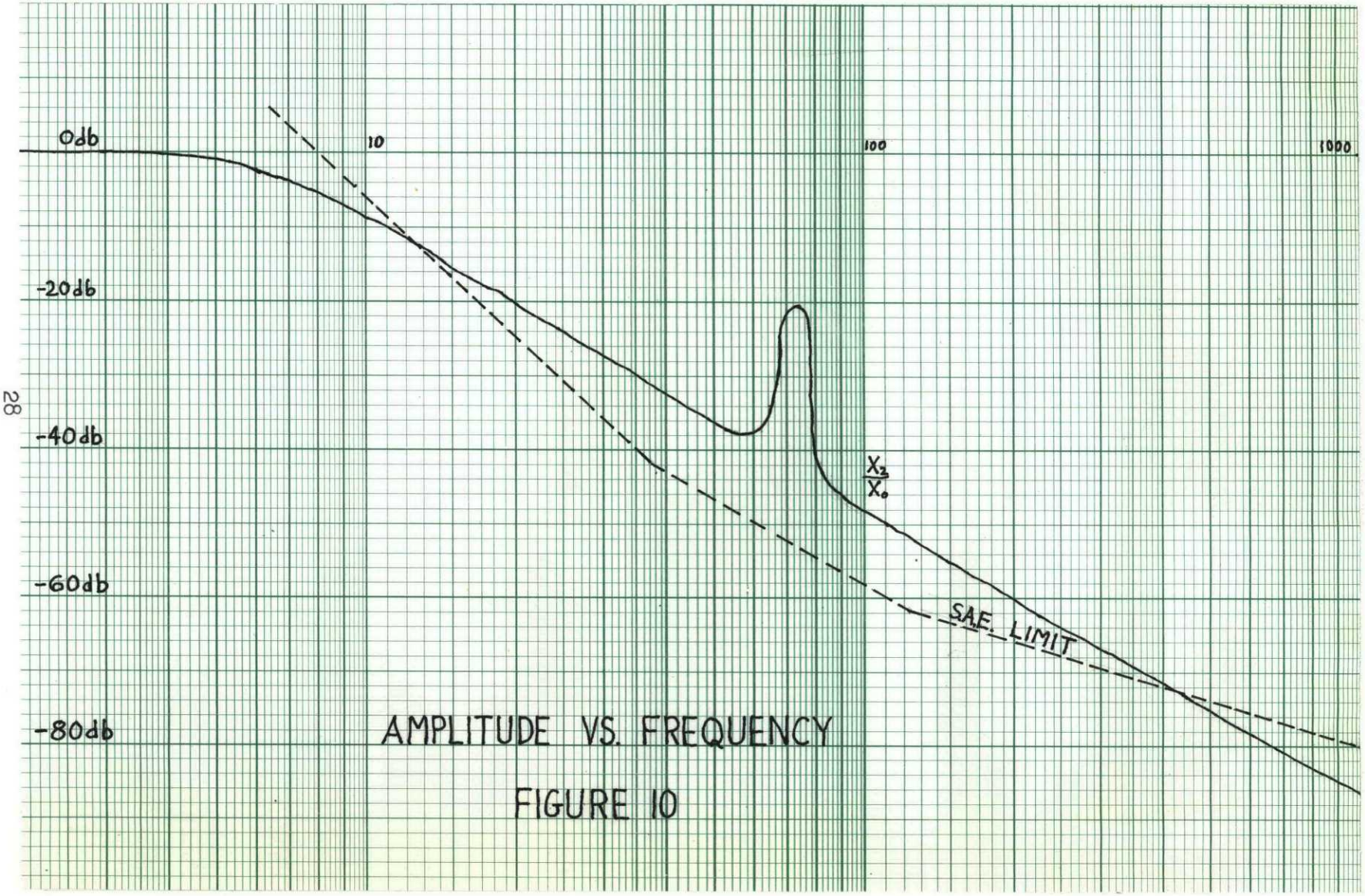

AMPLITUDE VS. FREQUENCY

FIGURE 10

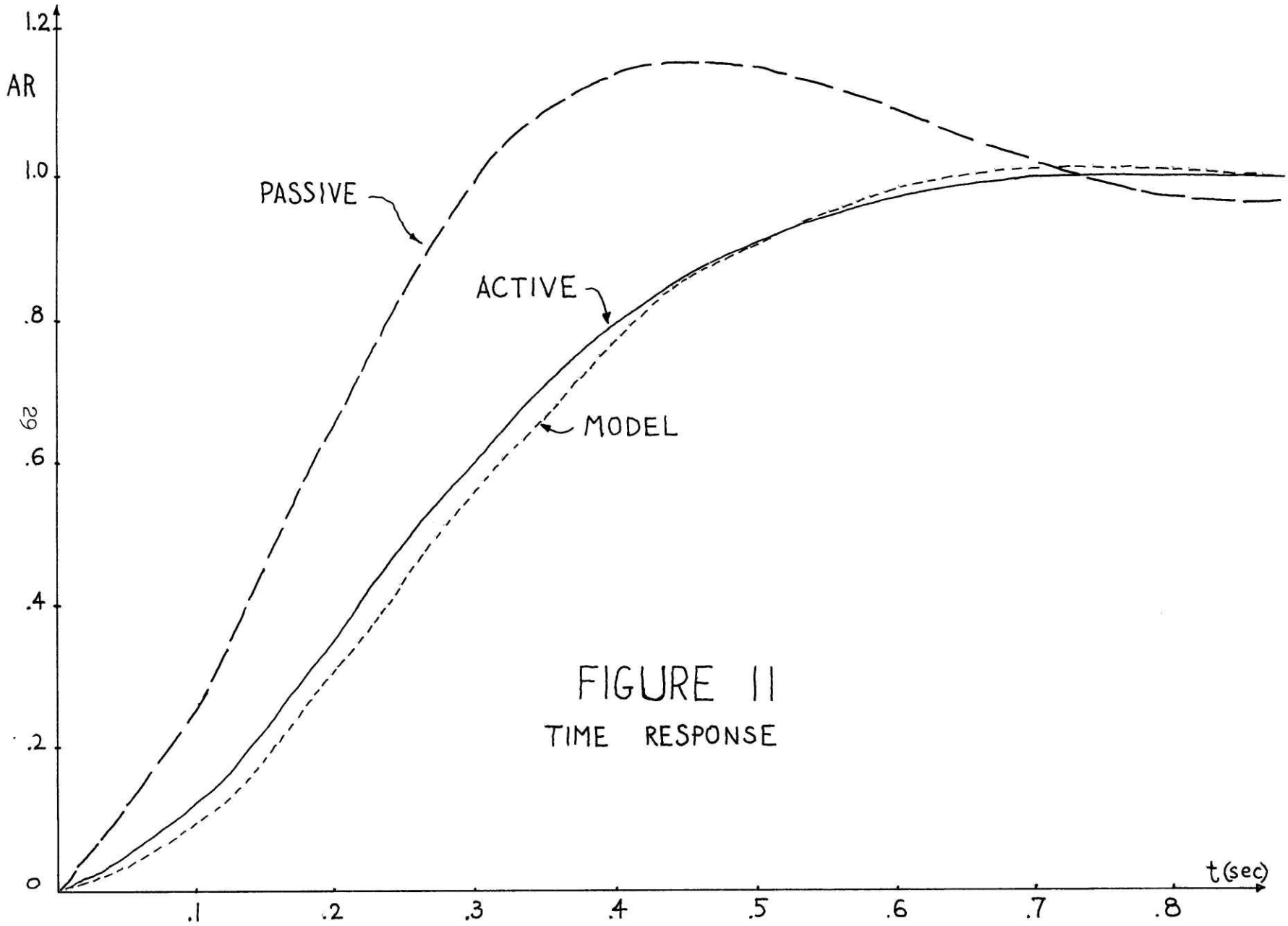

FIGURE 11

TIME RESPONSE

the axle acceleration and body rate were next introduced and similarly optimized with the previous parameters. The resulting frequency response is plotted in Fig. 12. Though the low frequency response was maintained, a slight increase in the resonant peak occurred. Moreover, the reduction in the amplitude which occurred at frequencies above has little effect on the system response. It was found that the use of acceleration feedback from the body deflections (C_4), reduced the high frequency resonance peak, but greatly deteriorated the low frequency component, as is evident in Fig. 13. Therefore, since the addition of acceleration and body deflection rate feedbacks had little effect near the wheel-bounce frequency, the initial design is more practical.

The resonant peak at the wheel-bounce frequency is an invariant point in the response curve. Due to the fact that it contains no natural damping, any damping that is added through active elements is at the expense of the low frequency response. X_2 is directly related to the spring and damper force; therefore, is the transmission X_2/X_0. Because the designer is forced to place the actuator between the two masses, along with the spring and damper, it is constrained by Newton's law. No force, regardless of the feedback information, can be introduced into only the first loop. The amplitude ratio at the resonance frequency of the tire is therefore not a function of the force coupling devices between the two masses. It is given simply by the ratio M_1/M_2, since the dynamic tire excitation is given by (4):

$$\frac{X_1 - X_0}{X_0} \simeq \frac{-M_1 s^2 \left[1 + M_2/M_1 (X_2/X_0)\right]}{M_1 s^2 + K_1} \qquad (4.44)$$

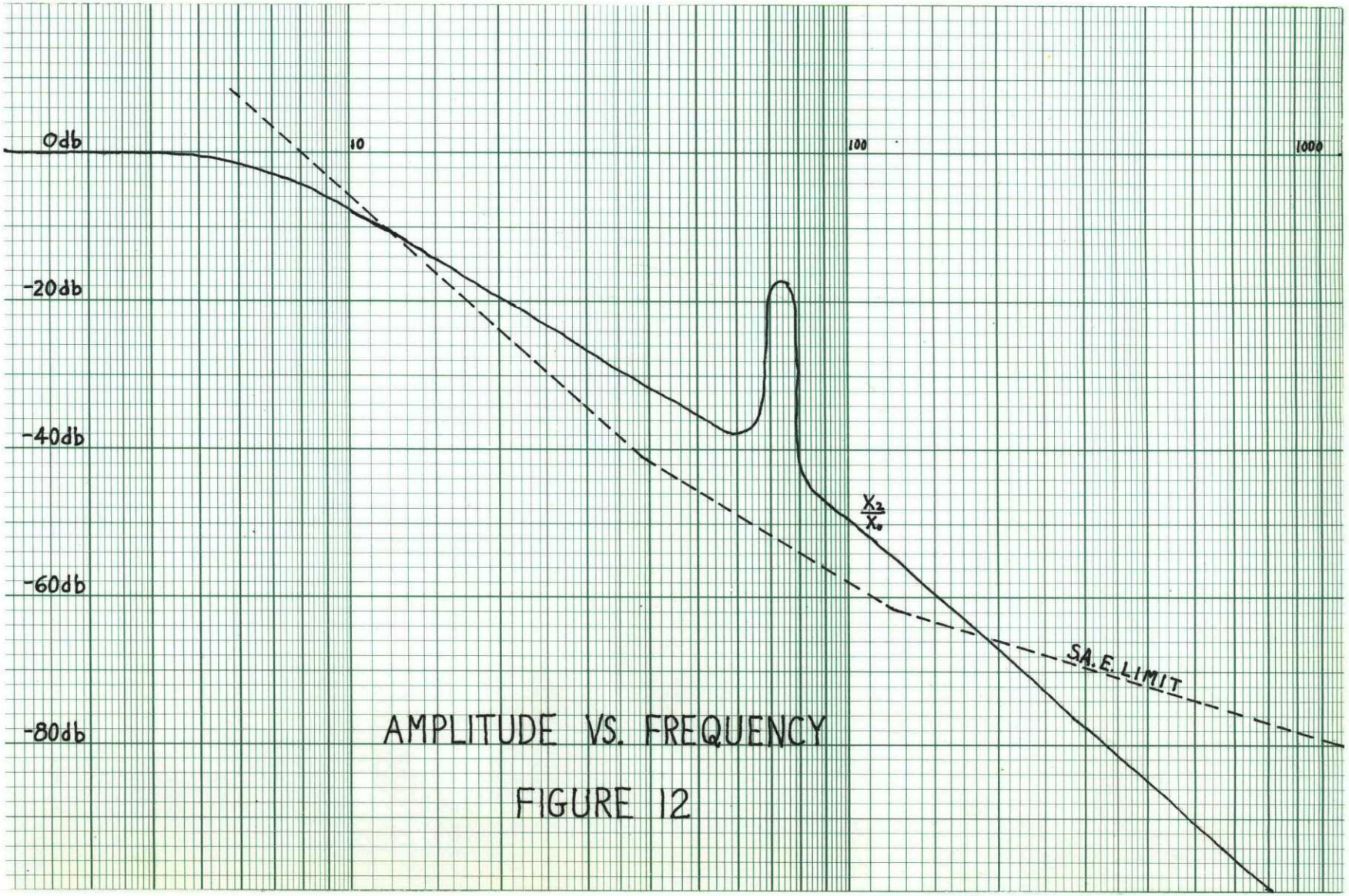

AMPLITUDE VS. FREQUENCY

FIGURE 12

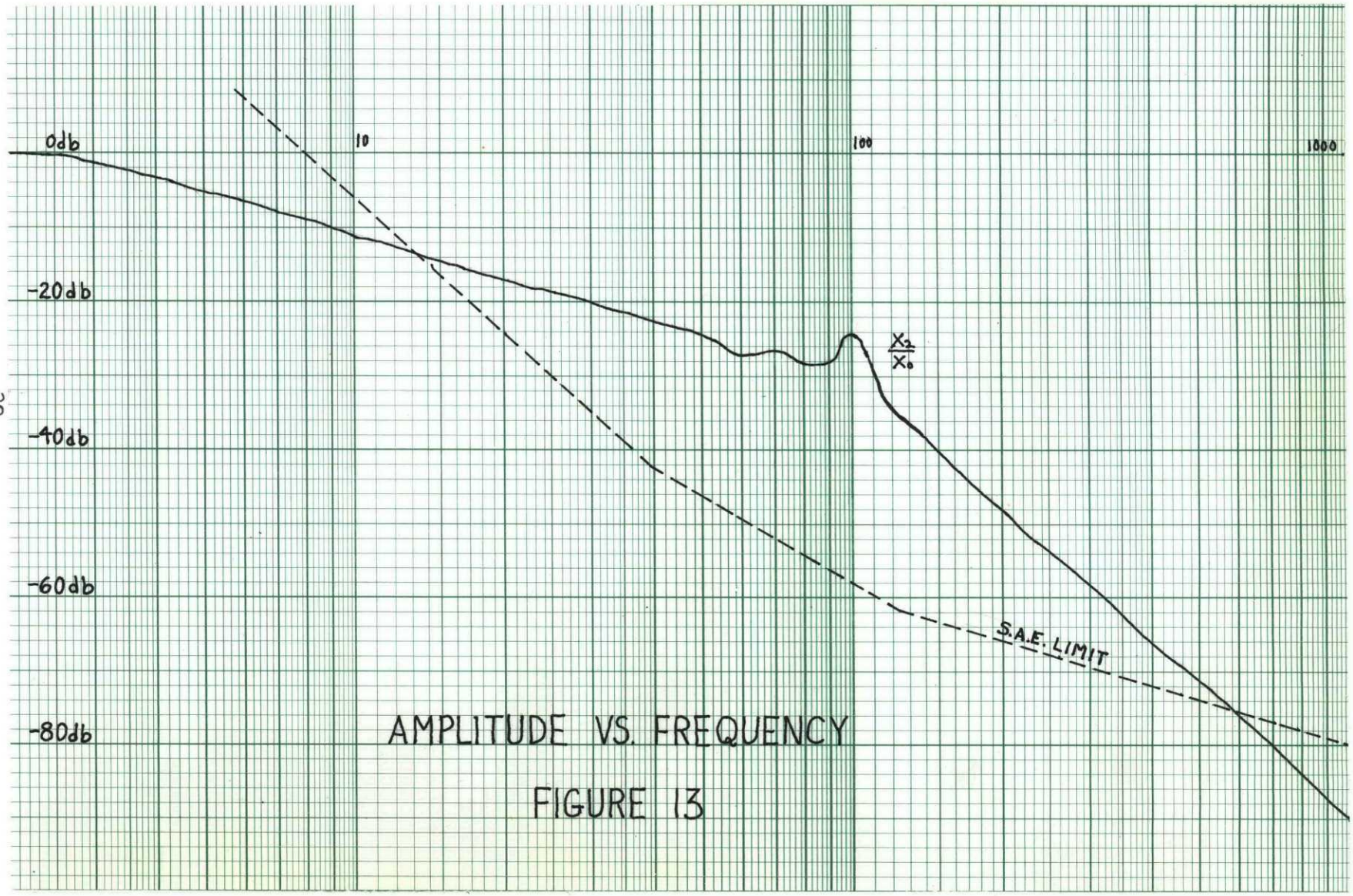

AMPLITUDE VS. FREQUENCY

FIGURE 13

From Fig. 10., the resonant peak rises approximately 22 db at ω_2 with active control in the suspension. However, it remains at the constant amplitude of -20 db, and this reduction is substantial.

One may conclude, that for road disturbances at the wheel-bounce natural frequency, the use of an active element offers no advantage in reducing the transmitted vibration. However, these disturbances are random, and the amplitude in the range of frequencies below the wheel-bounce frequency are greatly attenuated.

CHAPTER V

NONLINEAR ACTIVE SUSPENSION

One of the most important characteristics of nonlinear systems is that the response behavior is dependent upon the magnitude and type of input (11). For example, a nonlinear system may behave completely different in response to step inputs of different magnitudes. The effects of these phenomenon are often employed to improve a system's performance. The feasibility of employing a nonlinearity in the design of active suspensions is investigated in this chapter.

It is evident, that an automobile experiences a greater acceleration upon striking a sudden bump (positive step), than for a sudden dip (negative step) of the same magnitude, considering gravity forces. Although a rigorous analysis of this effect would involve the complete suspension system and its interactions, much can be determined from the single wheel model used previously. However, in analyzing the system response to step inputs, the wheel dynamics must account for the loss of contact with the road. This condition is certain to occur during dips or negative steps. Since the effective spring of the tire obviously contributes no force when this occurs, a constant limit must exist for negative values of the road input when loss of contact has occurred. This constant acceleration force may be modeled as in Fig. 14.

The application of nonlinear components in suspension systems is not new; having been employed in the design of shock absorbers. Most shock absorbers possess unsymmetric rates of compression and expansion. Pressure sensitive orifices regulate the leakage flow through the ram

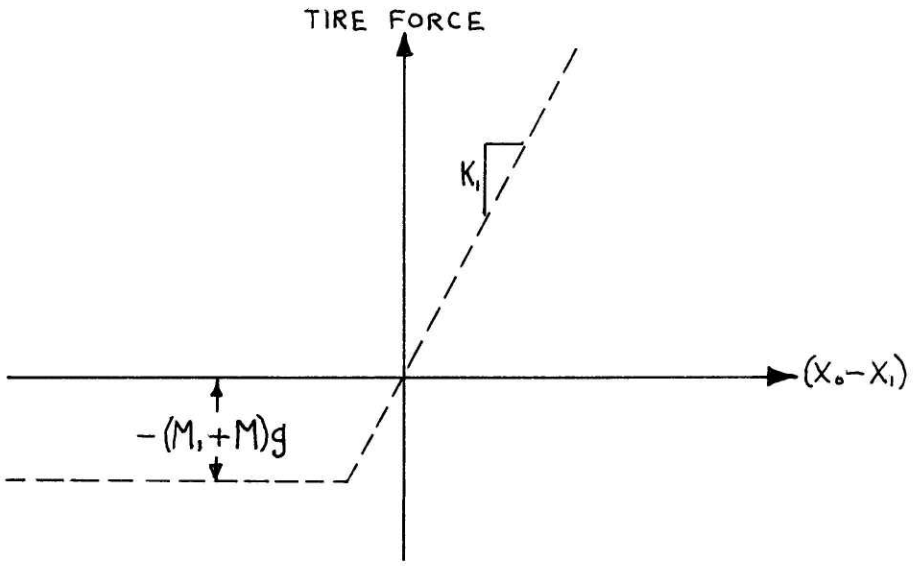

FIGURE 14

upon loading. Though it exhibits unintentional nonlinearities, a greater isolation from more severe road disturbances does render it practical. Numerous studies have been carried out on nonlinear damping forms, and it has been shown (5) that the optimum ratio of the damping rates for expansion to compression is about 3.5.

The unsymmetrical shock absorber has the obvious constraint of generating only forces opposite to the direction of motion and directly proportional to the deflection rate. This factor leads to the concept of producing optimum counterforces for sudden bumps and dips by means of the hydraulic actuator. As developed in Chapter III, the force output of the actuator is symmetric with respect to positive and negative input currents due to the conditions of constant electrical gain, symmetric port widths, and equal effective ram areas. For the nonlinear actuator, the ram areas on each side of the piston may be left as parameters. In

fact, a more practical design may be realized by employing a supporting rod on only one side, thus, increasing the other area. The unsymmetrical effect could be produced by different port areas in the spool, however, this condition would produce a steady state force since the underlap areas would be unequal.

In this nonlinear investigation, use is made of the analog computer. The suspension system and actuator can be simulated through its differential equations developed in Chapter IV. The effects of various parameter changes may be easily analyzed by way of potentiometer settings. Due to the large magnitudes in the equations of motion, both amplitude scaling and time scaling were required. A factor of 10 is suitable for the time scale to slow the problem down, and the amplitude scale factors are given in the Appendix. The automobile parameters, actuator parameters, and feedback constants are expressed as gains through the potentiometer settings and are also evaluated in the Appendix . The complete analog simulation, with a generation of the integral-square body acceleration is diagramed in Fig. 15. The active elements are controlled by switch S_1, a positive and negative step by S_2, and a linear versus nonlinear actuator by S_3.

First, the actuator was modeled as a separate linear gain for positive and negative inputs. Its characteristics are shown in Fig. 16. From the simulation in Fig. 15., the total gain may be adjusted by potentiometer 20, and the positive input gain only by potentiometer 21. By adjustment of these two gains, a minimum integral-square body acceleration was found. These optimum gains are given in Fig. 16., and the cor-

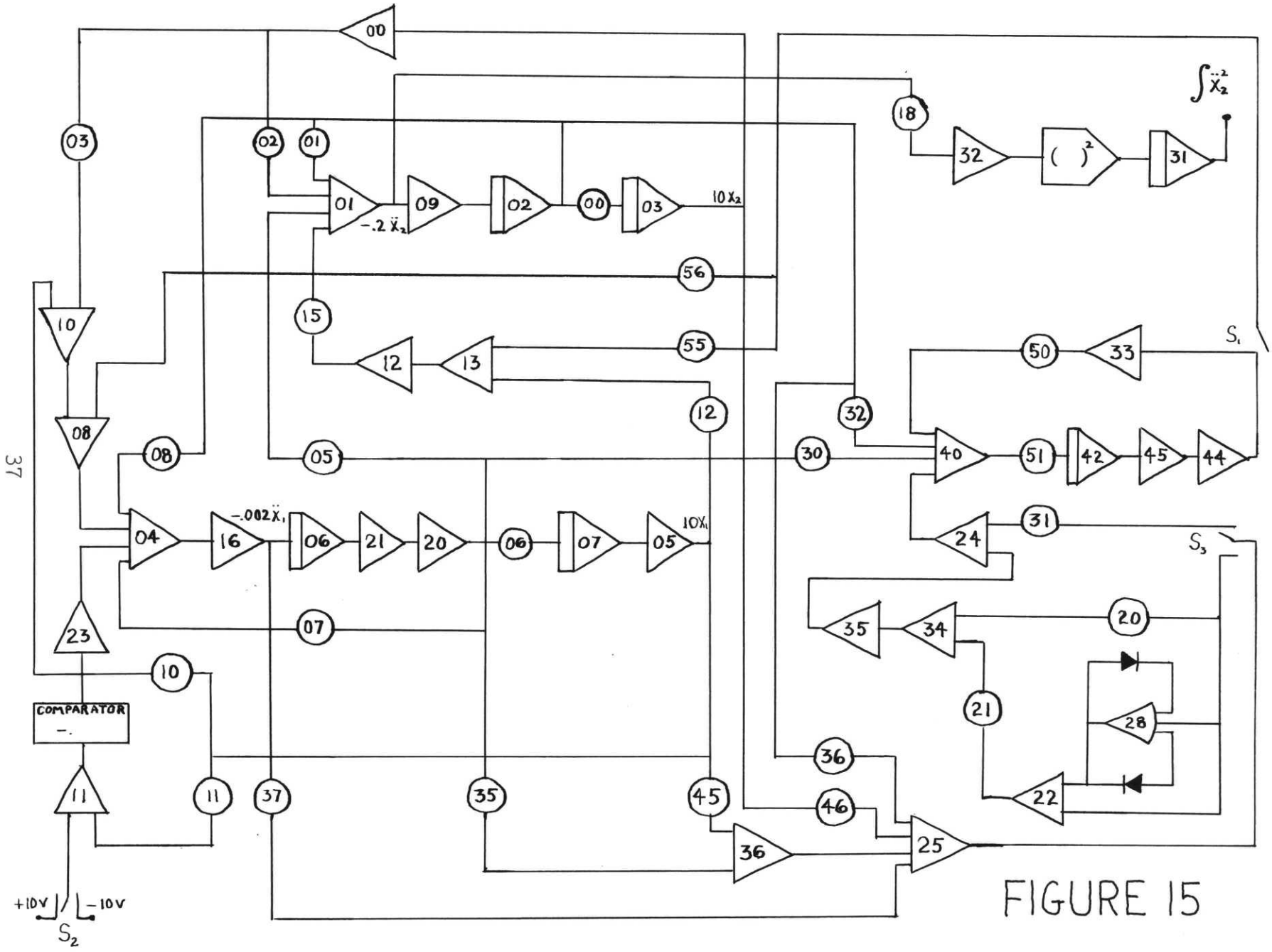
00
03
02
01
01
09
02
00
03
10 X2
-.2 X2
56
15
10
12
13
55
08
08
05
04
16
-.002 X1
06
21
20
06
07
05
10 X1
07
23
10
COMPARATOR
11
11
37
35
45
36
+10V
-10V
S2
18
32
( )2
31
50
33
S1
32
30
40
51
42
45
44
31
24
S3
35
34
20
21
28
22
36
46
25

FIGURE 15

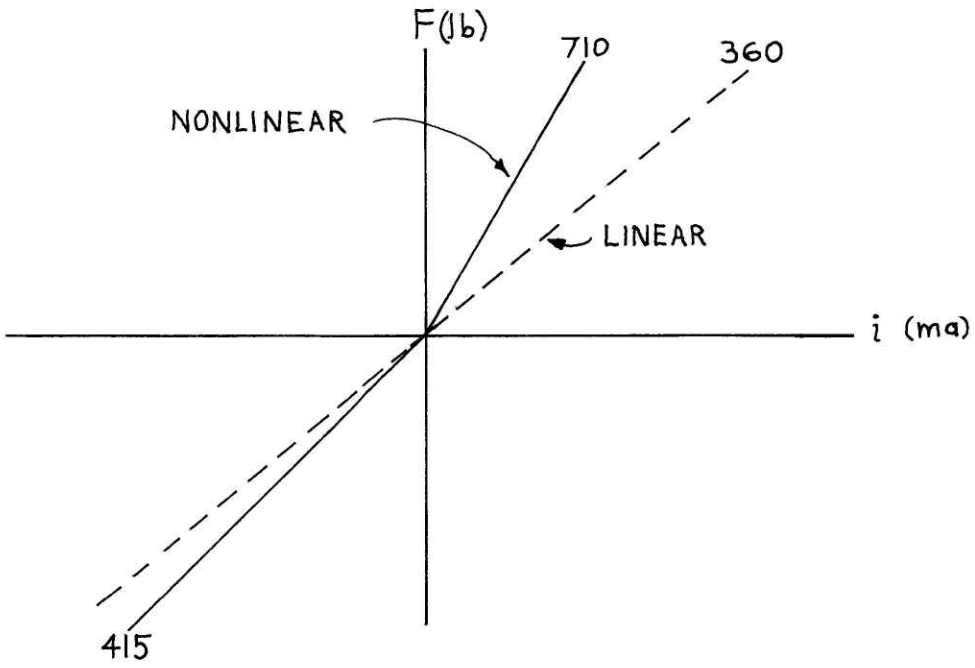

FIGURE 16

responding plots of the integral-square acceleration in Fig. 17. The actuator gain for negative inputs which minimized this variable was found to be 415 lb/ma, and the gain for positive inputs, to be 710 lb/ma as compared to a gain of 360 lb/ma found in Chapter IV. From Fig. 17., the integral-square body acceleraton was computed. For positive steps of 4 inches, a reduction of approximately 33% occurred; whereas for negative steps, the reduction was approximately 17%.

As an exploratory study of isolating large disturbances, the feedbacks for the actuator were chosen in an attempt to completely cancel out the spring and damper forces on the body mass. Therefore, the position difference, and the rate difference in the deflections of the body and axle were sensed, and fedback with gains equal to the spring K_2 and damping C_1+B respectively. However, complete cancellation of these forces


LINEAR
POSITIVE STEP
NONLINEAR
LINEAR
NEGATIVE STEP
NONLINEAR

FIGURE 17

for large magnitudes would induce stability problems. Therefore, the actuator was modeled with a saturation limit. Fig. 18. represents this force cancellation and limit on the actuator force. A simple diode circuit was used to limit the actuator force.

Fig. 19. shows the body and axle response of the passive system to positive and negative steps of 3 inches. In Fig. 20., the response of the active system with feedback gains equal to the spring and damping constants is shown. By adjusting the saturation limits, a very good cancellation may be obtained for a step input, however, a step in the opposite direction caused great overshoot, and an offset steady state value. In Fig. 20., a negative step of 3 inches is absorbed, almost entirely, as is evident from the body deflection. The corresponding positive step caused a rise in the body deflection of approximately 6 inches

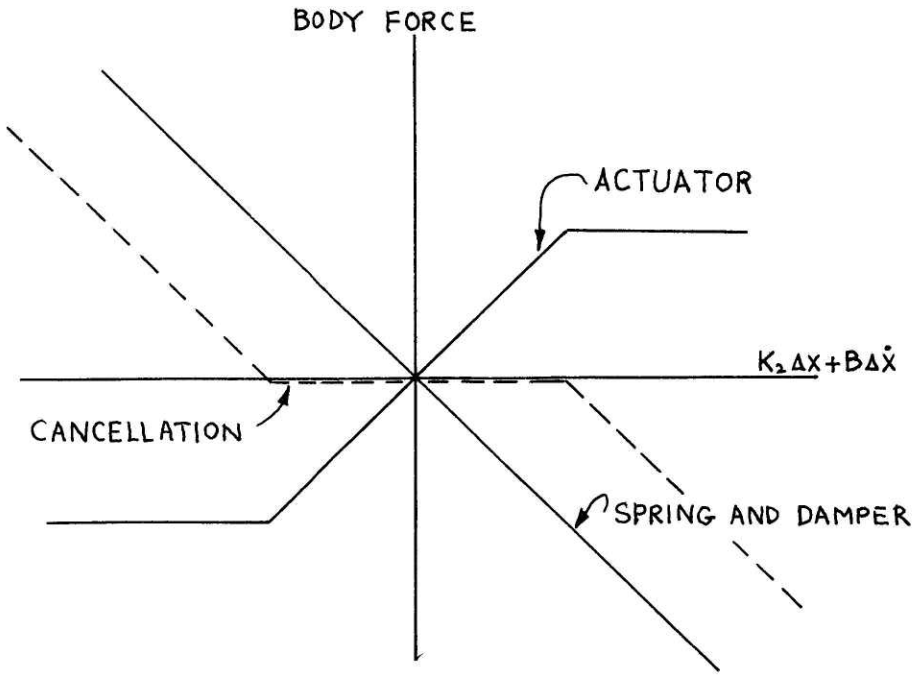

FIGURE 18

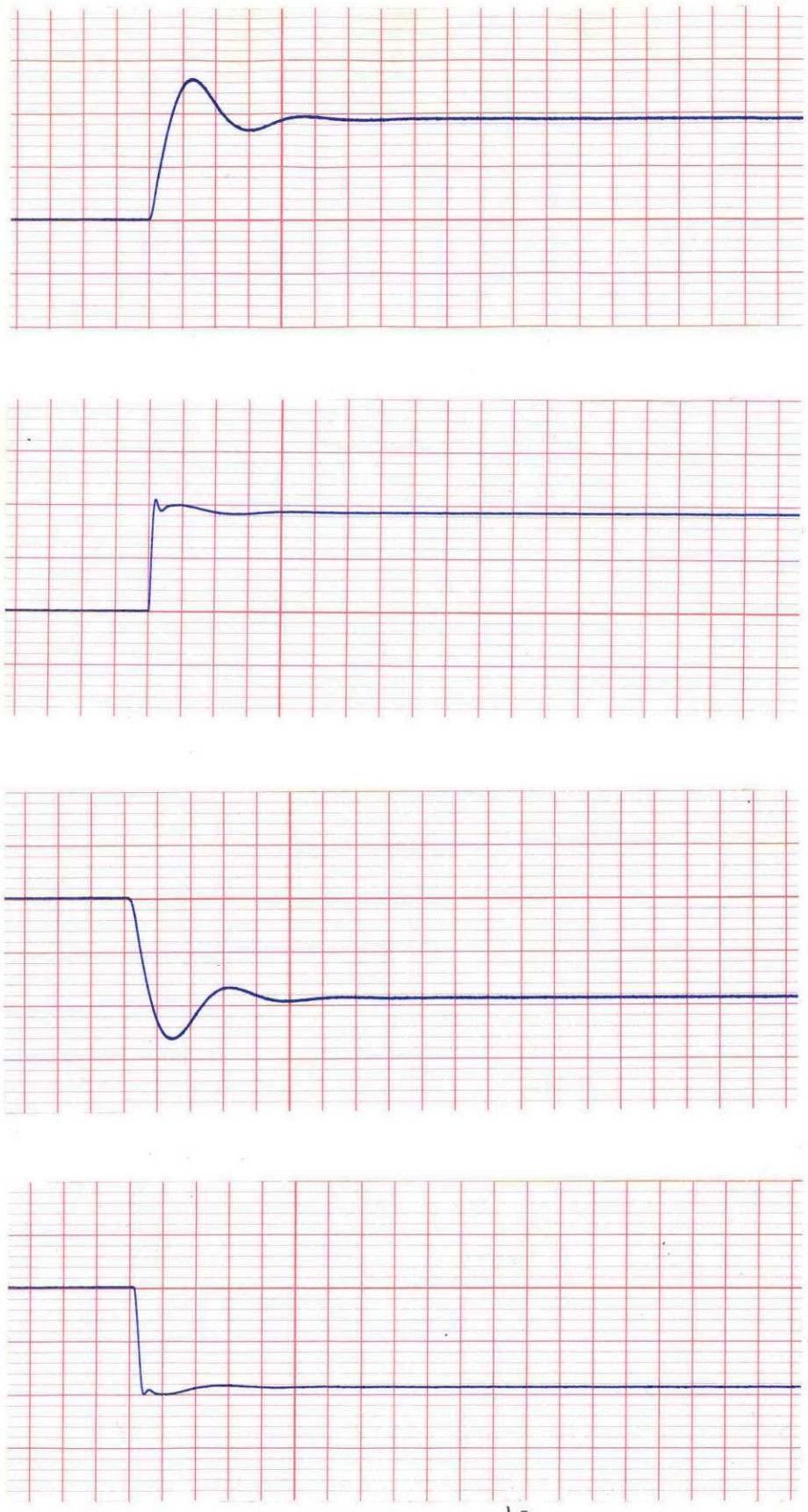

FIGURE 19

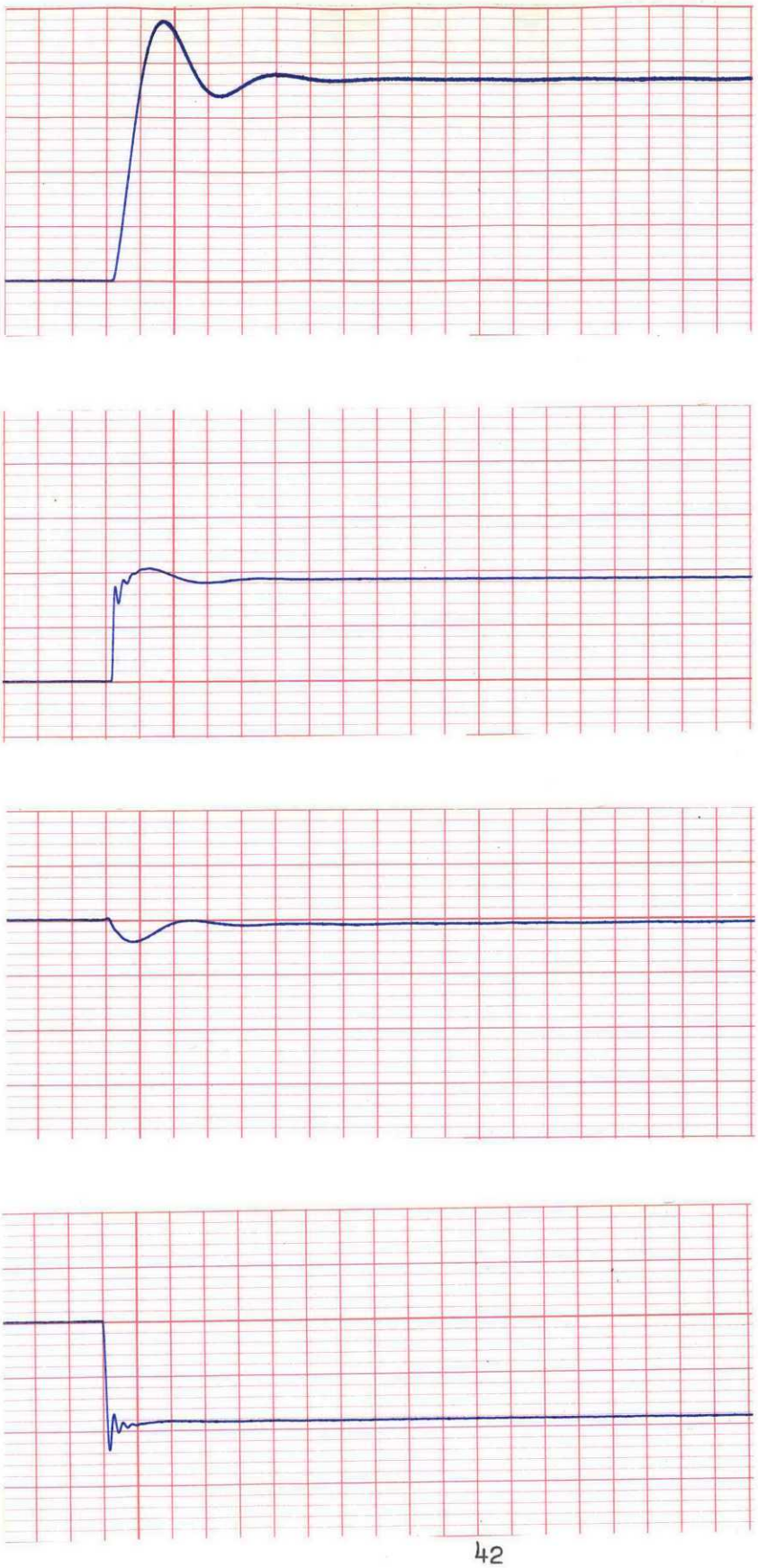

FIGURE 20

or a 3 inch steady state value. The optimum response of the active system for both positive and negative steps has little improvement over that of the passive system, as may be observed in Fig. 21. The corresponding plots of body acceleration are shown in Fig. 22. The initial peak acceleration from the impact with the step was reduced very little, but a reduction in the mean value did occur.

Cancellation of disturbing forces on the body is theoretically a feasible method of obtaining a very smooth ride over rough terrain. The asymmetry exhibited in the tire model however, reveals that further unsymmetrical forces are needed. Possible signal compensation techniques could also be investigated. By approximate cancellation of the forces at all frequencies, the effective spring and damper are greatly reduced, resulting in a lightly damped low frequency system. Therefore, the application of filtering to cancel high frequency disturbances is a reasonable investigation.

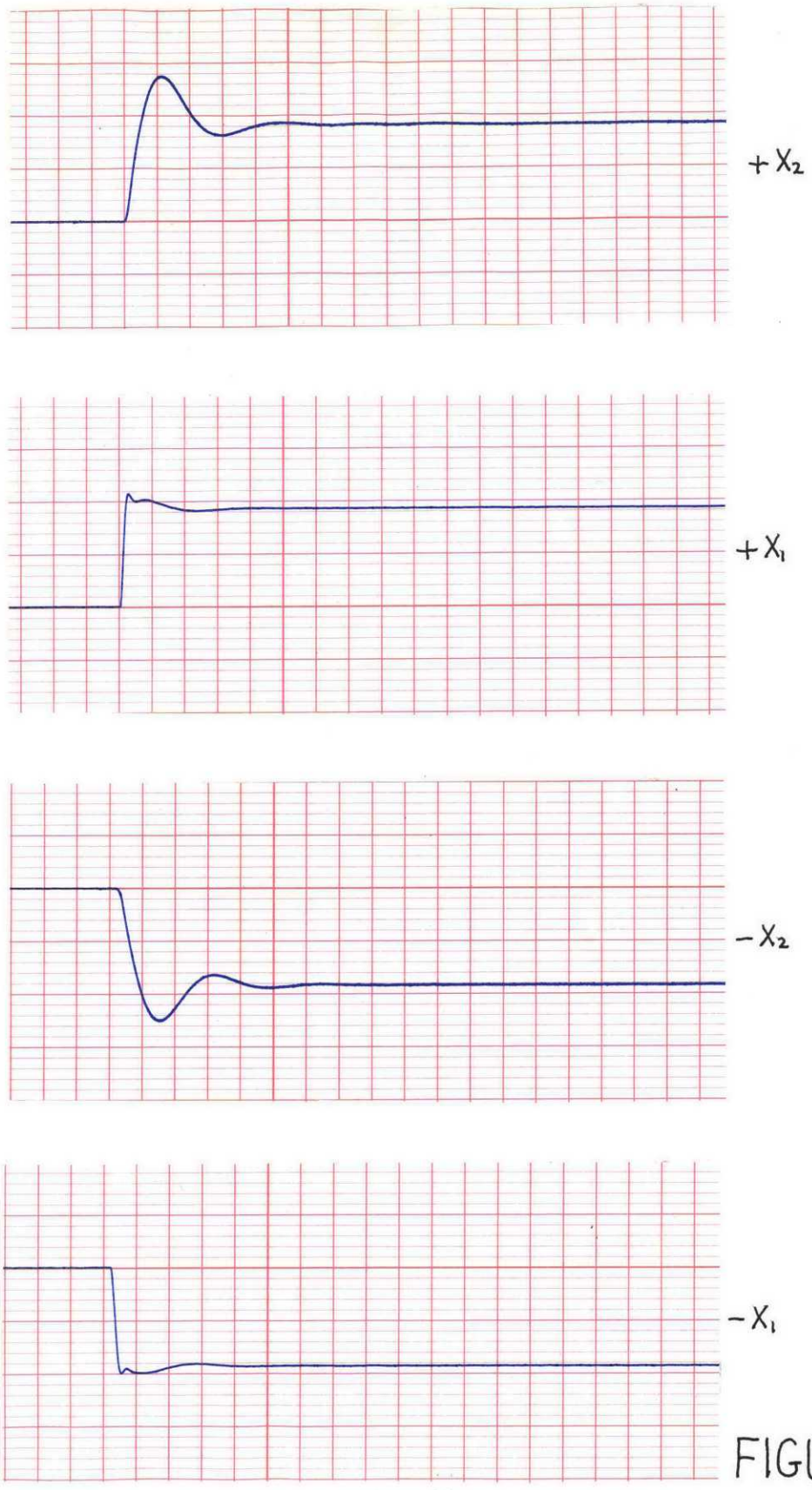

FIGURE 21

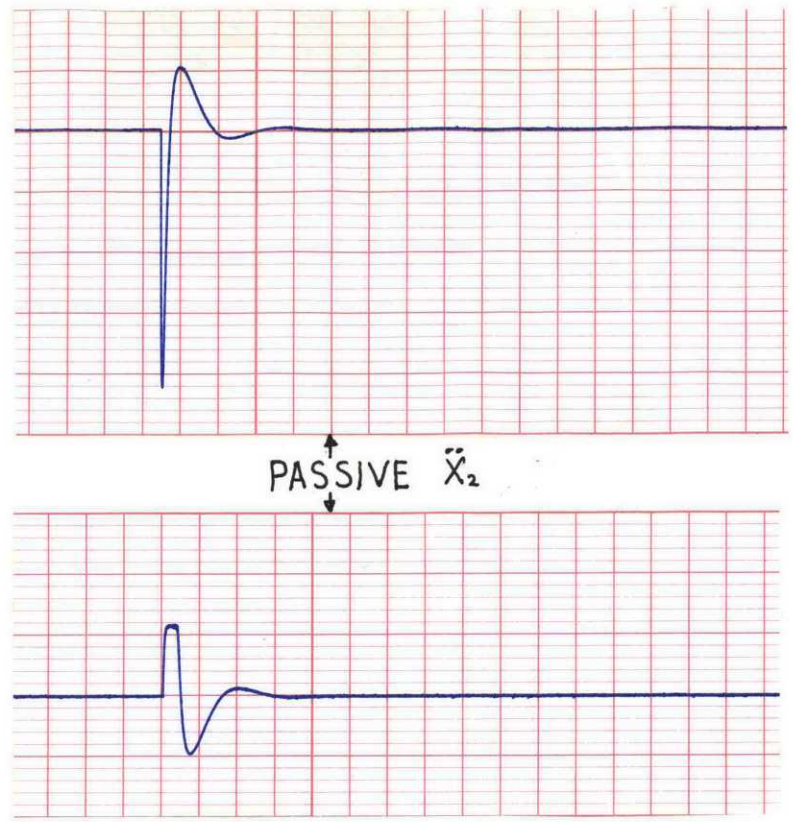

FIGURE 22

CHAPTER VI

CONCLUSIONS

The results have shown that body vibrations from road disturbances can be effectively reduced by the application of active elements into the suspension system. Electrohydraulic actuators may be designed with existing components to meet transmission requirements, and are particularly well suited for such an application. By a proper choice of driving signals to the actuator, it can be made to produce both spring and damping forces, thus altering the system damping and natural frequencies. Though ride quality is a subjective measurement, comfortable transmission limits can be related to amplitude-frequency information. By the use of computer programs to find the optimum values for feedback signals and actuator parameters, the system may be designed by way of its amplitude-frequency characteristics.

In the linear design of Chapter IV, the feedback signals consisted of the acceleration of both masses, the velocity of both masses, their difference, and the rate of their difference. At the natural wheel-bounce frequency, the vibration transmission could not be decreased due to physical constraints, without a great increase in the low frequency range. However, for frequencies below this, the active system proved very effective.

The effect of nonlinear force characteristics may be useful in the isolation of large, discrete disturbances. Because the tire leaves the road, the force generated into the suspension system is asymmetric with respect to positive and negative step inputs. The suspension system

with the feedback parameters found in the linear analysis was modeled on the analog computer in order to investigate this condition. The actuator was then altered to produce adjustable forces for positive and negative inputs corresponding to each of the two conditions. It was found through studies of the integral-square body acceleration, that a substantial decrease with positive steps could be realized with this nonlinearity.

As an exploration into sustaining zero-induced acceleration on the automobile body, rate and displacement between the two masses corresponding to the spring and damping constants were used to drive the actuator. By forcing the wheel to follow the road, the actuator would then completely cancel out the spring and damping forces. Thus, the body position would remain constant, even though the wheel, for example, experienced a sudden rise or fall. Though the cancellation could not be made complete, within saturation limits, for both positive and negative steps, it could be accomplished separately with different saturation limits. The method is feasible; although further investigations into signal compensation techniques and additional nonlinearities to affect the unsymmetrical response was not possible in this study. However, if interest in this possibility has been stimulated, it has served a purpose.

APPENDIX

PROBLEM VARIABLE	MAXIMUM EXPECTED VALUE	SCALE FACTOR	COMPUTER VARIABLE
X_2	10/12 ft	120/10 > 10 volts/ft	$10X_2$
X_1	10/12 ft	120/10 > 10 volts/ft	$10X_1$
$\dot{X}_2$	5 ft/sec	10/5 ≥ 2 volts/ft/sec	$2\dot{X}_2$
$\dot{X}_1$	50 ft/sec	10/50 ≥ .2 volts/ft/sec	$.2\dot{X}_1$
$\ddot{X}_2$	50 ft/sec^2	10/50 ≥ .2 volts/ft/sec	$.2\ddot{X}_2$
$\ddot{X}_1$	5000 ft/sec^2	10/5000 ≥ .002 volts/ft/sec	$.002\ddot{X}_1$
F	2000 lb	10/2000 ≥ .005 volts/lb	.005 F
X_0	CONSTANT		
$\dot{F}$	41,500 lb/sec	10/41,500 ≥ 10^{-4}(2.4) volts/lb/sec	.00024 $\dot{F}$

G = LINEAR ACTUATOR GAIN

P00 = $5/\beta$

P01 = $B/M_2\beta$

P02 = $K_2/5M_2\beta$

P03 = $K_2/50M_1\beta$

P04 = 0

P05 = $B/M_2\beta$

P06 = $5/\beta$

P07 = $B/10M_1\beta$

P08 = $B/10M_1\beta$

P10 = $K_2/50M_1\beta$

P11 = $K_1/500M_1\beta$

P12 = $K_2/50M_2\beta$

P13 = $K_1X_0/500M_1\beta$

P15 = $1/10$

P18 = $5/\beta$

P30 = $C_1/100$

P31 = $G/500$

P32 = $C_1/1000$

P35 = $C_3/72$

P36 = $C_5/720$

P37 = $C_2/.72$

P45 = $C_6/3600$

P46 = $C_6/3600$

P50 = .40

P51 = .208

P55 = $2/\beta$

P56 = $.2/\beta$

REFERENCES

1. Calcaterra, P., Cavanaugh, R., Schubert, D., Study of Active Vibration Isolation Systems For Severe Ground Transportation Environments. NASA Contractor Report CR-1454. Barry Wright, Inc., Watertown, Mass., November 1969.

2. Panzer, M., "The theory and synthesis of active suspension systems", Dissertation (D.E.E.), Polytechnic Institute of Brooklyn, 1960, University Microfilms, Inc., Mic. 59-6747.

3. Bender, E.K., Karnopp, D.C., and Paul, I.L., "On the optimization of vehicle suspensions using random process theory", A.S.M.E. Publication 67-tran-12, 1967.

4. Thompson, A.G., "Design of Active Suspensions", Proc. Instn. Mech. Engrs., Vol. 185 36/71, 1970.

5. Thompson, A.G., "Optimum damping in a randomly excited non-linear suspension", Vol. 184 pt. 2A No. 8., Proc. Inst. Mech. Engrs., 1969-70.

6. Ride and Vibration Data, S.A.E. Publication S.P.-6, 1950.

7. Lewis, E., and Stern, H., Design of Hydraulic Control Systems. McGraw-Hill, 1962.

8. Blackburn, J., Reethof, G., and Shearer, J., ed., Fluid Power Control. M.I.T. Technology Press and Wiley and Sons, 1960.

9. Corsetti, C., Dillow, J., A Study of the Practibility of Active Vibration Isolation Applied to Aircraft During the Taxi Condition. Technical Report AFFDL-TR-71-159. Wright-Paterson Air Force Base, Ohio: Air Force Flight Dynamics Laboratory, Systems Command, July 1972.

10. Whitaker, H. Philip, The System Description Program, Revision 1. Measurement Systems Laboratory RE-79, Massachusetts Institute of Technology. September 1972.

11. Ogata, K., Modern Control Engineering. Englewood Cliffs, N.J., Prentice Hall, Inc., 1970.